Title
Gonadotropin regulation of glutamate cysteine ligase catalytic and modifier subunit expression in rat ovary is subunit and follicle stage specific

Journal
AJP Endocrinology and Metabolism, 289(3)

ISSN
0193-1849

Authors
Tsai-Turton, Miyun
Luderer, Ulrike

Publication Date
2005-09-01

DOI
10.1152/ajpendo.00531.2004

Am J Physiol Endocrinol Metab 289: E391–E402, 2005.
First published April 5, 2005; doi:10.1152/ajpendo.00531.2004.

Gonadotropin regulation of glutamate cysteine ligase catalytic and modifier subunit expression in rat ovary is subunit and follicle stage specific

Miyun Tsai-Turton[1] and Ulrike Luderer[1,2,3]

Departments of [1]Community and Environmental Medicine, [2]Medicine, and [3]Developmental and Cell Biology, University of California at Irvine, Irvine, California

Submitted 4 November 2004; accepted in final form 26 March 2005

Tsai-Turton, Miyun, and Ulrike Luderer. Gonadotropin regulation of glutamate cysteine ligase catalytic and modifier subunit expression in rat ovary is subunit and follicle stage specific. *Am J Physiol Endocrinol Metab* 289: E391–E402, 2005. First published April 5, 2005; doi:10.1152/ajpendo.00531.2004.—We have observed that levels of the antioxidant glutathione (GSH) and protein levels of the catalytic and modifier subunits of the rate-limiting enzyme in GSH synthesis, GCLc and GCLm, increase in immature rat ovaries after treatment with gonadotropin. The goals of the present studies were to delineate the time course and intraovarian localization of changes in GSH and GCL after pregnant mare's serum gonadotropin (PMSG) and after an ovulatory gonadotropin stimulus. Twenty-four hours after PMSG, there was a shift from predominantly granulosa cell expression of *gclm* mRNA, and to a lesser extent *gclc*, to predominantly theca cell expression. GCLc immunostaining increased in granulosa and theca cells and in interstitial cells. Next, prepubertal female rats were primed with PMSG, followed 48 h later by 10 IU of hCG. GCLm protein and mRNA levels increased dramatically from 0 to 4 h after hCG and then declined rapidly. There was minimal change in GCLc. The increase in *gclm* mRNA expression was localized mainly to granulosa and theca cells of preovulatory follicles. To verify that GCL responds similarly to an endogenous preovulatory gonadotropin surge, we quantified ovarian GCL mRNA levels during the periovulatory period in adult rats. *gclm* mRNA levels increased after the gonadotropin surge on proestrus and then declined rapidly. Finally, we assessed the effects of gonadotropin on ovarian GCL enzymatic activity. GCL enzymatic activity increased significantly at 48 h after PMSG injection and did not increase further after hCG. These results demonstrate that gonadotropins regulate follicular GCL expression in a follicle stage-dependent manner and in a GCL subunit-dependent manner.

glutathione; γ-glutamylcysteine synthetase; preovulatory gonadotropin surge

THE TRIPEPTIDE GLUTATHIONE (GSH, γ-glutamylcysteinylglycine) and its related enzymes are involved in many cellular functions. GSH, alone and in concert with the enzyme glutathione peroxidase, maintains cellular redox status by reducing reactive oxygen species (ROS) like hydrogen peroxide (5). In the process, GSH is oxidized to glutathione disulfide (GSSG). Under normal conditions, GSSG is reduced back to GSH by the action of glutathione reductase, maintaining the intracellular levels of GSH far in excess of GSSG. However, under conditions of excessive production of ROS, this system can be overwhelmed. GSH conjugation, catalyzed by enzymes of the glutathione-*S*-transferase family, is also an important detoxification mechanism for many xenobiotics. For example, the reactive metabolites of the potent ovarian toxicants cyclophosphamide and polycyclic aromatic hydrocarbons are detoxified by GSH conjugation (9, 18, 42).

The ovary depends on de novo synthesis to maintain intracellular GSH. GSH is synthesized in two sequential, ATP-dependent enzymatic reactions that are catalyzed by glutamate cysteine ligase (GCL, also called γ-glutamylcysteine synthetase) and glutathione synthetase, respectively. The GCL holoenzyme is composed of a catalytic (GCLc) subunit and a modifier (GCLm) subunit (11, 45). GCLc has all substrate binding sites and possesses the catalytic activity of the GCL enzyme. GCLm does not have any catalytic activity but modulates the affinity of GCLc for substrates and inhibitors. De novo synthesis of GSH can be regulated by transcriptional and posttranscriptional regulation of GCL, by the availability of cysteine, and by negative feedback of GSH on GCL, resulting in decreased enzymatic activity (11, 45).

Although uncontrolled production of ROS can result in oxidative stress and damage to cells, ROS may also function as signaling molecules. Within the rat ovary, levels of superoxide anion increase and enzymatic activity of superoxide dismutase falls on the day of estrus (23). Moreover, administration of exogenous superoxide dismutase blocks ovulation (41). Leukocytes appear to be the major source of superoxide anion within the ovary during the periovulatory period (22), and infusion of leukocytes into perfused rat ovaries enhances the LH-stimulated ovulation rate (14). ROS in the ovary may also arise as byproducts of cellular respiration and of steroid synthesis, as they do in other steroidogenic tissues (15, 36). Adverse effects of ROS have been demonstrated in ovarian cells. Hydrogen peroxide interferes with normal granulosa cell function, decreasing the cAMP and progesterone responses to FSH stimulation (29). ROS may also play a role in follicular apoptosis. Follicles in serum-free culture spontaneously undergo apoptosis within hours (49). This can be prevented by FSH or by antioxidants, including the GSH precursor *N*-acetylcysteine (49). Gonadotropin administration to prepubertal rats in vivo also inhibits granulosa cell apoptosis (48), upregulates ovarian expression of the antioxidant genes manganese superoxide dismutase and secreted superoxide dismutase (28, 49), and increases ovarian levels of GSH and GCL subunit protein (3, 28). Together, these data suggest that ovarian antioxidants, and particularly GSH, must be tightly regulated to maintain ROS-dependent signaling pathways without allowing oxidative stress to occur.

We (28) previously reported that ovarian GSH concentrations and GCL subunit protein levels increase during the first

Address for reprint requests and other correspondence: U. Luderer, Center for Occupational and Environmental Health, Univ. of California, Irvine, 5201 California Ave., Suite 100, Irvine, CA 92617 (e-mail: uluderer@uci.edu).

The costs of publication of this article were defrayed in part by the payment of page charges. The article must therefore be hereby marked "*advertisement*" in accordance with 18 U.S.C. Section 1734 solely to indicate this fact.

24 h of follicular growth induced by pregnant mare's serum gonadotropin (PMSG), before any increase in ovarian GCL mRNA levels. The goals of the present studies were *1*) to further delineate the time course of changes in ovarian GCL subunit expression after PMSG, *2*) to localize GCL subunit protein and mRNA within the ovary after PMSG administration, *3*) to investigate the effects of an ovulatory gonadotropin stimulus on ovarian GCL protein and mRNA expression, and *4*) to investigate the effects of PMSG and an ovulatory gonadotropin stimulus on GCL enzymatic activity.

METHODS

Animals

Female Sprague-Dawley rats [Crl:CD(SD)IGS BR] were obtained from Charles River Laboratories (Wilmington, MA). Upon arrival, the animals were housed in an American Association for the Accreditation of Laboratory Animal Care-accredited facility, 3 or 4 to a cage, with free access to deionized water and standard laboratory chow, on a 14:10-h light-dark cycle. The experimental protocols were carried out in accordance with the *Guide for the Care and Use of Laboratory Animals* (33) and were approved by the Institutional Animal Care and Use Committee at the University of California, Irvine.

Experimental Protocols

Effect of PMSG priming on ovarian GCL subunit protein and mRNA expression levels and intraovarian localization. Twenty-five-day-old female rats were injected subcutaneously with 10 IU of PMSG (obtained from Dr. A. F. Parlow, Director, National Institute of Diabetes and Digestive and Kidney Diseases National Hormone and Peptide Program) in sterile 0.9% sodium chloride to stimulate ovarian follicular development or saline alone. PMSG possesses both FSH and LH activity in the rat (25). At 4, 8, 24, and 48 h after injection, animals were euthanized by decapitation for collection of trunk blood, and both ovaries were dissected out. Body weights at the time the animals were killed ranged from 45.5 to 87 g. These time points were chosen because we had previously observed statistically significant increases in whole ovary GCLm protein levels in this time frame (28). In the present study, the combined whole ovary GCL subunit protein, GCL subunit mRNA, and GSH data from the present experiment and the previous study (Ref. 28; with permission of the publisher) are presented together so that the time course of changes in these parameters can best be appreciated. Ovaries were processed for one of several assays as follows. For GSH assay, one ovary was immediately homogenized on ice in 1:6 (wt/vol) 5% sulfosalicylic acid and centrifuged at 15,800 *g*, and supernatants were stored at −70°C (n = 4–14 ovaries/group). For protein extraction and Western analysis (n = 6–9 ovaries/group) or for RNA extraction and Northern analysis (n = 5–12 ovaries/group), ovaries were immediately frozen on dry ice and stored at −70°C. For immunohistochemistry (n = 6 ovaries/group) or in situ hybridization (n = 6 ovaries/group), the ovary was pre-fixed in 4% paraformaldehyde in PBS for 1 h at 4°C, dehydrated in 15% sucrose in PBS for 3–4 h at 4°C, embedded in Tissue Tek OCT (Sakura Finetek, Torrance, CA), and stored at −70°C until sectioning at 10-μm thickness using a cryostat. Ovaries were serially sectioned, and every fourth serial section was processed for GCLc immunohistochemistry. Adjacent sections were processed for in situ hybridization for *gclc* or *gclm*.

Effect of ovulatory dose of human chorionic gonadotropin on whole ovary GCL protein and mRNA expression and intraovarian localization of GCL mRNA in PMSG-primed rats. Female rats (23–24 days old) weighing 41.5–58 g were injected subcutaneously with 10 IU of PMSG. Forty-eight hours later, some of the rats were killed by carbon dioxide asphyxiation followed by decapitation for collection of trunk blood. The remaining rats were injected subcutaneously with 10 IU of human chorionic gonadotropin (hCG; CG-10, Sigma-Aldrich, St. Louis, MO) in PBS and were killed 4, 6, or 12 h later. Unlike PMSG, hCG possesses exclusively LH activity in the rat (34). Ovaries were processed for GSH assay (n = 5–11 ovaries/group), protein extraction for Western analysis (n = 5–10 ovaries/group), RNA extraction for quantification by real-time PCR (n = 3–8 ovaries/group), or in situ hybridization (n = 2–3 ovaries/group) as above. *gclc* and *gclm* in situ hybridization was performed in three separate experiments, each including two or three slides probed with antisense riboprobe and one slide probed with sense riboprobe for each subunit from each ovary, as well as "positive control" kidney sections.

Effect of endogenous gonadotropin surge on GCL expression in the ovary. Nine- to ten-week-old adult female rats weighing 202–269 g that had displayed at least two 4-day estrous cycles, as determined by daily vaginal cytology, were killed by carbon dioxide anesthesia followed by decapitation for collection of trunk blood *1*) at 0900 on proestrus; *2*) at 2200 on proestrus evening, ~4 h after the preovulatory surge; *3*) at 0000 on estrus, ~6 h after the surge; and *4*) at 0900 on estrus morning, ~15 h after the surge (n = 4 at each time point). Carbon dioxide asphyxiation was carried out in the dark, with only safelight illumination for the 2200 and 0000 hour time points to avoid disrupting the animals' light-dark cycles. One ovary was processed for GSH assay, and one ovary was processed for RNA extraction as described above.

Effect of PMSG and hCG on ovarian GCL enzymatic activity. Female rats (23–24 days old) weighing 48.5 to 63 g were injected subcutaneously with 10 IU of PMSG at 0800 or 1200 or with saline vehicle at 1200 (n = 8/group). The animals treated with PMSG at 0800 were injected subcutaneously with 10 IU of hCG 48 h after PMSG. All animals were killed by carbon dioxide asphyxiation followed by decapitation for collection of trunk blood at 1200 on the second day after injection (48 h after PMSG or saline or 4 h after hCG). The timing was chosen so that GCL activity assays could be done immediately upon removal of the ovaries. Ovaries were homogenized on ice in 1:6 (wt/vol) TES-SB buffer (20 mM Tris, 1 mM EDTA, 250 mM sucrose, 20 mM boric acid, 2 mM L-serine). An aliquot of homogenate was snap-frozen for subsequent protein assay. The remaining homogenate was immediately used for GCL enzymatic activity assay.

Total GSH and Oxidized GSH Assays

Total GSH and oxidized GSH (GSSG) were measured using the enzymatic recycling method (12). 2-Vinylpyridine (Sigma-Aldrich) was used to remove reduced GSH from aliquots of sample, permitting the measurement of GSSG (12). GSSG assay was carried out on separate aliquots of the supernatants from 5% sulfosalicylic acid tissue homogenates used for the total GSH assay. Supernatants (25 μl) were diluted 1:1 with GSH assay buffer (143 mM Na_2HPO_4, 6.3 mM EDTA, pH 7.5). Standards of GSSG (Sigma-Aldrich) were also prepared in 1:1 GSH assay buffer-5% sulfosalicylic acid. The resulting 50 μl of sample or standard were mixed with 7 μl of triethanolamine (diluted 1:10 with deionized water) to a pH of 5.5–7.0. Four microliters of 2-vinylpyridine were added per tube, and the tubes were vortexed for 1 h at room temperature. Sixty microliters of chloroform were added per tube. The tubes were vortexed again for 15 min and were then centrifuged at 15,800 *g* for 5 min at 4°C. Five microliters of the aqueous phase from samples or standards were pipetted in triplicate into a 96-well microplate. Thirty-three microliters of water were added per well, and the plate was incubated at 30°C for 10 min. Next, a 162-μl reaction mixture containing 0.26 mM NADPH, 0.74 mM 5,5′-dithiobis(2-nitrobenzoic acid), and 0.62 U/ml glutathione reductase (all from Sigma-Aldrich) were added to each well, and the absorbance was monitored at 412 nm every 10 s for 30 min using a VersaMax Tunable Microplate Reader (Molecular Devices, Sunnyvale, CA). The assay protocol for total GSH was identical to that of the GSSG assay from the step at which 5 μl of sample or standard

were pipetted in triplicate into a 96-well microplate, except that the absorbance was monitored for only 90 s. The interassay coefficient of variation (CV) for total GSH in a rat liver pool was 12.2%; the intra-assay CVs ranged from 4.0 to 5.3%. For GSSG, the interassay CV was 6.8%, and the intra-assay CVs for the two assays for this experiment were 3.9 and 2.3%. The sensitivity of these assays in our hands is 0.015 nmol.

Northern Analysis

RNA extraction, RNA gel electrophoresis, and Northern Blotting for *gclc*, *gclm*, and *gapdh* were carried out as described (28). Total ovarian RNA was prepared using the TRIzol reagent (Life Technologies, Gaithersburg, MD) according to the manufacturer's instructions. Samples of RNA were analyzed by separation in 1% agarose-formaldehyde-containing gels, followed by capillary transfer to nylon membranes and hybridization with ^{32}P-labeled nucleic acid probes. ^{32}P-labeled random-primed probes were prepared using template full-length cDNAs of the mouse *gclc*, *gclm* (38, 39), and *gapdh* (Ambion, Austin, TX) genes with the DECAprime II DNA Labeling Kit (Ambion). Visualization was by autoradiography. Semiquantitative analysis of autoradiographs was performed using a Stratagene molecular documentation and image analysis system with EagleSight software. Ovarian *gclc* absorbance readings and the mean of the absorbance readings for the two *gclm* transcripts were normalized to control mRNA (*gapdh*) and relative differences among treatment groups were calculated.

Fluorogenic 5′-Nuclease mRNA Quantitation (Real-Time PCR)

RNA was extracted using TRIzol reagent (Invitrogen Life Technologies, Carlsbad, CA) according to the manufacturer's instructions. Two micrograms of RNA from each sample were incubated for 30 min at 37°C with DNAse I (0.25 U), dithiothreitol (10 mM), and RNAse inhibitor (10 U) and then inactivated at 70°C. Oligo(dT)$_{15}$ primer (0.13 μg, Invitrogen) was added and the mixture incubated at 70°C for 5 min. Finally, reverse transcription was carried out by adding RT Master Mix containing Superscript II RNase H-Reverse Transcriptase (100 U), dNTPs (1.43 mM), first-strand buffer, and dithiothreitol (14.3 mM; all from Invitrogen) at 45°C for 1 h. RT reactions were shipped on dry ice to the University of Washington, where fluorogenic 5′-nuclease assays (TaqMan) were carried out using an ABI Prism 7700 sequence detection system (PerkinElmer Applied Biosystems). The thermal cycling conditions comprised an initial denaturation step at 95°C for 10 min, followed by 40 cycles at 95°C for 20 s and 62°C for 60 s. The gene-specific sequences of all primer pairs and probes used in the TaqMan assays are listed in Table 1. The PCR primers and the dual-labeled probes were designed using the primer design software Primer Express (PerkinElmer Applied Biosystems). The specific PCR primers and/or the corresponding dual-labeled probes were designed to span intron/exon boundaries, thus eliminating spurious results derived from DNA-contaminated RNA samples. Synthesis of probes was performed by IDT (Coralville, IA). Probes were labeled at the 5′ end with the fluorescent molecule 6-carboxyfluorescein (6-FAM) and at the 3′ end with the quenching molecule 6-carboxytetramethylrhodamine (TAMRA). A standard curve derived from serial dilutions of rat kidney RNA was used to determine concentrations of the *gclc* and *gclm* mRNAs normalized to *gapdh*.

Table 1. *Primer pairs and probes used in real-time PCR assays*

cDNA, GenBank Acc. No.	Type of Oligo	Sequence
gclc	Primer (forward)	atgtggacacccgatgcagtatt
J05181	Primer (reverse)	tgtcttgcttgtagtcaggatggttt
	Probe (antisense)	ttctccagatgctctcttct
gclm	Primer (forward)	gccaccagatttgactgccttt
NM_017305	Primer (reverse)	cagggatgctttcttgaagagctt
	Probe (antisense)	ctctgaggcaagtttcca
gapdh	Primer (forward)	tcctgcaccaccaactgctt
NM_017008	Primer (reverse)	gaggggccatccacagtctt
	Probe (antisense)	ggctcatgaccacagtccatgccatcac

gclc and *gclm*, catalytic and modifier glutamate cysteine ligase, respectively; *gapdh*, glyceraldehyde-3-phosphate dehydrogenase.

Western Analysis

Protein extraction, gel electrophoresis, and Western blotting for GCLc, GCLm, and β-actin were carried out as described (28). Briefly, 40 μg of protein extract from each ovary were loaded onto polyacrylamide gels, separated by electrophoresis, transferred to PVDF membranes, blocked, and incubated with GCLm and GCLc antisera (47). Blots were subsequently reprobed with β-actin antiserum (Sigma-Aldrich) as a loading control. The second antibody was horseradish peroxidase-conjugated goat antirabbit (for GCLc and GCLm) or antimouse (for β-actin) immunoglobulin G (Amersham Pharmacia Biotech, Piscataway, NJ). Visualization was accomplished using enhanced chemiluminescence (ECL, Amersham Pharmacia Biotech) followed by exposure to Hyperfilm ECL (Amersham). Semiquantitative analysis of films was performed using a Stratagene molecular documentation and image analysis system with EagleSight software.

In Situ Hybridization

In situ hybridization for *gclc* and *gclm* was adapted from Wilcox et al. (51) as previously described (27). Briefly, ^{35}S-labeled antisense and sense riboprobes were transcribed from full-length 0.82-kb mouse *gclm* cDNA in pCR II (39) or a 0.6-kb mouse *gclc* cDNA fragment in pBluescript II (20). Sections were postfixed in 4% paraformaldehyde, treated with proteinase K, and prehybridized before hybridization overnight at 55°C with 3×10^6 cpm/slide of the appropriate riboprobe. Sections of kidney were used as "positive controls" because of the known high levels of GCL subunit mRNA in this organ (24). Negative control slides were incubated with sense *gclc* or *gclm* riboprobes.

Serial sections of ovaries were examined under bright- and dark-field microscopy. At least eight slides per ovary, each with eight sections, were evaluated in a blinded manner, and the evaluator's impressions of the intensity of hybridization in the granulosa cells, theca cells, and oocytes of each follicle class [primary (Pederson stages 1–3), secondary (Pederson stages 4–5), or antral (Pederson stages 6–8) (35, 37)] were recorded. The reported changes were consistently observed between three or more in situ hybridization runs.

Immunohistochemistry

Immunohistochemistry was performed using a polyclonal rabbit anti-GCLc and the Vectastain ABC Kit (Vector Laboratories, Burlingame, CA). This antibody has previously been shown to be specific for GCLc (6). The GCLm antibody used for Western blotting was not useful for immunohistochemistry. For antigen retrieval, slides were heated at high power in a conventional microwave oven in 1 mM sodium citrate and 1 mM citric acid buffer for 3 min. The slides were blocked with 3% hydrogen peroxide in methanol for 10 min, 1.5% goat serum in PBS for 20 min, and avidin D-biotin blocking solution (Vector Laboratories) for 15 min each. The slides were incubated with primary antibody (1:1,000) in PBS for 90 min, washed, incubated with biotinylated goat anti-rabbit IgG in PBS for 30 min, washed, incubated with ABC reagents for 30 min, washed, and incubated with diaminobenzidene substrate for 8 min. Finally, the slides were counterstained with hematoxylin, dehydrated in graded ethanol washes, washed in xylene, and mounted with Permount (Fisher Scientific, Pittsburgh, PA). Kidney sections were used as positive controls

because GCLc is highly expressed in the paracortical region of the kidney. Negative controls were incubated with nonimmune rabbit serum without primary antibody.

Serial sections of ovaries were examined in a blinded manner under light microscopy. Follicles were classified and impressions of the intensity of immunostaining were recorded as described for in situ hybridization.

Estradiol and Progesterone Assays

Estradiol and progesterone radioimmunoassays were performed as previously described (26). All samples were assayed in duplicate. The progesterone assay utilized the Progesterone CL Radioimmunoassay Kit (Diagnostic Systems, Webster, TX). The interassay CV for a high-progesterone rat serum pool was 9.6%; the intra-assay CV was 4.3%. The sensitivity of the assay is 7.5 pg. For the estradiol assay, a standard curve was prepared in charcoal-stripped, ovariectomized rat serum by use of a stock solution of 17β-estradiol (Sigma) dissolved in 100% ethanol at a concentration of 100 ng/ml that was serially diluted to concentrations of 7.8, 15.6, 62.5, 125, 250, 500, and 1,000 pg/ml. The other reagents were from the Estradiol Double Antibody Radioimmunoassay Kit (Diagnostic Products, Los Angeles, CA). All of the estradiol measurements for the present studies were done in one assay. The intra-assay CV was 4.9%. The sensitivity of this assay is 1.6 pg.

GCL Enzymatic Activity Assay

GCL activity was measured essentially as described by White et al. (50). Ovaries homogenized in TES-SB buffer (20 mM Tris, 1 mM EDTA, 250 mM sucrose, 2 mM L-serine, 20 mM boric acid) were centrifuged, and the supernatant was diluted again in TES-SB for a final dilution of 1:24 (wt/vol). Fifty microliters of sample (in duplicate) or GSH standards in TES-SB were added to prewarmed 1.5-ml microcentrifuge tubes containing GCL reaction cocktail (in mM: 400 Tris, 40 ATP, 20 L-glutamic acid, 2 EDTA, 20 boric acid, 2 L-serine, 40 $MgCl_2$) in a 37°C water bath. After 11 min of preincubation, the reaction was initiated by the addition of 50 μl of 2 mM L-cysteine to one of each of the two sample tubes. After exactly 20 min of incubation, the reaction was stopped by the addition of 50 μl of 200 mM sulfosalicylic acid to all tubes. Then, 50 μl of cysteine were added to the second tube for each sample (the baseline GSH tube) and to the standard tubes. Samples were vortexed, incubated on ice for 20 min, and centrifuged at 1,800 *g* at 4°C for 5 min. Twenty microliters of supernatant (in triplicate) were pipetted into the wells of a 96-well microplate. One hundred eighty microliters of NDA solution (1.4 parts 50 mM Tris base, pH 10, 0.2 parts 0.5 N NaOH; 0.2 parts 10 mM 2,3-naphthalenedicarboxaldehyde in DMSO) were then added to each well. The plate was incubated at room temperature for 30 min and read at an excitation wavelength of 485 nm and emission wavelength of 530 nm in a Biotek FL600 spectrofluorometer microplate reader (Biotek Instruments, Winooski, VT). Results were expressed as nanomoles of GSH synthesized above the baseline GSH level per minute per milligram ovary or per milligram protein [determined using the Pierce BCA Protein Assay Kit (Pierce, Rockford, IL)]. The intra-assay CVs for the two assays for this experiment were 3.3 and 3.3%. The sensitivity of the assay in our hands is 0.10 nmol.

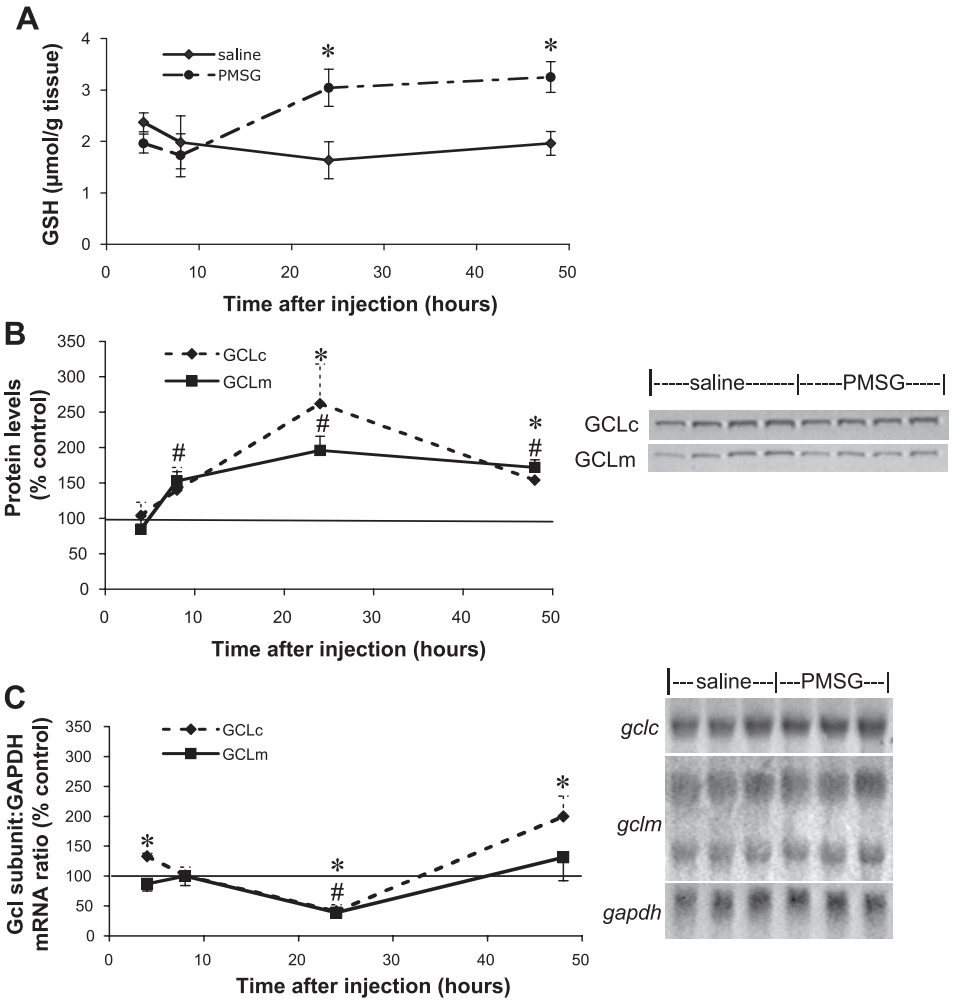

Fig. 1. Time course of change in ovarian glutathione (GSH) and glutamate cysteine ligase (GCL) subunit mRNA and protein levels after pregnant mare's serum gonadotropin (PMSG) or saline treatment. Prepubertal, 25-day old rats were injected sc with 10 IU PMSG in 0.9% NaCl or saline alone. Ovaries were removed at 4, 8, 24, or 48 h after injection and processed for GSH assay, protein extraction, and Western analysis or RNA extraction and Northern analysis, as detailed in MATERIALS AND METHODS. *A*: graph shows mean ± SE ovarian GSH concentrations in PMSG- and saline-treated animals ($n = 4$–14/group). *Significantly different from respective saline control, $P < 0.05$, by *t*-test. *B*: representative Western blot shows GCL subunits at 4 h after saline or PMSG. Graph shows mean ± SE catalytic (GCLc) or modifier (GCLm) GCL protein optical density expressed as %saline control for the same blot at indicated times after PMSG injection ($n = 6$–9/group). **gclc* Significantly different from respective saline control, $P < 0.05$; #*gclm* significantly different from respective saline control, $P < 0.05$. *C*: representative Northern blot shows GCL subunits and *gapdh* at 4 h after saline or PMSG. Graph shows mean ± SE *gclc* or *gclm* mRNA optical density normalized to *gapdh* and expressed as %control ($n = 5$–12/group). There are 2 *gclm* mRNA transcripts. Therefore, the sum of the 2 bands was normalized to *gapdh* for *gclm*. **gclc* Significantly different from respective saline control, $P < 0.05$; #*gclm* significantly different from respective saline control, $P < 0.05$. Some of the 8-, 24-, and 48-h data shown in these graphs were reported previously (28), used with permission from the publisher.

Statistical Analysis

Homogeneity of variances was assessed by Levene's test. When variances were not homogeneous, a natural logarithm transformation was applied. When variances remained inhomogeneous after transformation, a nonparametric test was used. Analysis of variance followed by Fisher's least significant difference test for determination of differences among groups was used to analyze differences among more than two groups. Alternatively, the Kruskal-Wallis test was used for nonparametric data. For comparisons of the means of two groups, the independent samples *t*-test for equal or nonequal variances, as appropriate, was used. Results were considered significantly different if $P < 0.05$. Statistical analyses were carried out using SPSS 11.0 for Macintosh OSX.

RESULTS

Effect of PMSG Priming on Ovarian GCL Subunit Protein and mRNA Expression Levels and Intraovarian Localization

Ovarian GSH concentrations and GCL subunit levels. Ovarian GSH concentrations were significantly higher at 24 and 48 h after PMSG treatment than with saline ($P < 0.001$, $P = 0.003$, respectively; Fig. 1*A*). Ovarian GCLm protein levels increased significantly by 8 h after PMSG and remained elevated relative to saline controls at 24 and 48 h ($P = 0.034$, $P = 0.002$, $P < 0.001$, respectively; Fig. 1*B*). There was no concomitant increase in *gclm* mRNA levels after PMSG. In fact, both *gclc* and *gclm* mRNA levels were significantly lower at 24 h after PMSG than at 24 h after saline ($P = 0.008$, $P = 0.003$, respectively). Ovarian GCLc protein levels were significantly increased at 24 h and 48 h after PMSG relative to saline ($P = 0.023$, $P = 0.018$; Fig. 1*B*). Ovarian *gclc* mRNA levels were 1.3-fold higher at 4 h after PMSG than at 4 h after saline ($P = 0.029$) and 2.0-fold higher at 48 h after PMSG than at 48 h after saline ($P = 0.027$; Fig. 1*C*).

Intraovarian localization of GCL expression. At 24 h after PMSG (Fig. 2, *B* and *D*) there was an overall increase in GCLc immunostaining in granulosa cells and theca cells that was not limited to a particular follicle class compared with saline controls (Fig. 2, *A* and *C*). GCLc immunostaining also increased in interstitial cells after PMSG.

In saline-treated animals, *gclm* mRNA was expressed predominantly in granulosa cells of growing follicles, whereas *gclc* mRNA was more ubiquitously expressed (Fig. 3, *B* and *F*). Atretic follicles had lower levels of *gclm* expression in granulosa cells (Fig. 3, *A* and *B*). After PMSG treatment, pronounced *gclm* expression appeared in the theca cells of the larger antral follicles, with less granulosa cell expression (Fig. 3*D*). In contrast, *gclm* mRNA expression remained high in the granulosa cells of smaller, growing follicles, while also appearing in the theca cells of those follicles after PMSG administration. Expression of *gclc* mRNA also became more prominent in theca cells after PMSG administration (Fig. 3*H*).

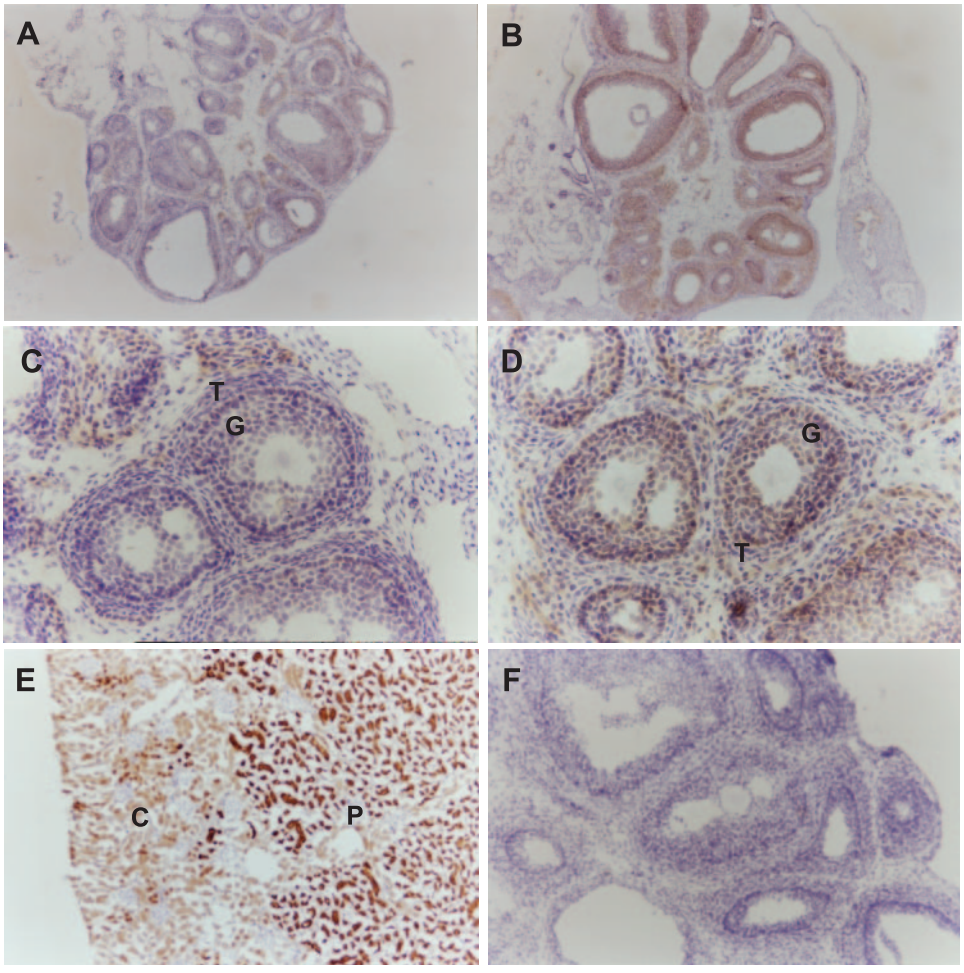

Fig. 2. Intraovarian localization of GCLc protein expression at 24 h after PMSG. Prepubertal 25-day-old rats were injected sc with 10 IU PMSG or saline vehicle and killed 24 h later. Ovaries were processed for immunohistochemistry for GCLc as detailed in MATERIALS AND METHODS. *A*: ovary from saline-treated animal shows faint GCLc antibody binding in granulosa cells and interstitial cells. Original magnification ×13.2. *B*: ovary from PMSG-treated animal shows more intense GCLc antibody binding in granulosa, theca, and interstitial cells. Original magnification ×13.2. *C*: secondary follicles in ovary of saline-treated animal. Original magnification ×66. *D*: secondary follicles in ovary of PMSG-treated animal show increased GCLc immunostaining in granulosa (G) and theca (T) cells compared with saline-treated animal in *C*. Original magnification ×66. *E*: "positive control" kidney section shows intense paracortical (P) GCLc immunostaining and lighter cortical (C) staining. Original magnification ×13.2. *F*: negative control ovary treated with nonimmune rabbit serum in place of GCLc antiserum shows no nonspecific binding. Original magnification ×33.

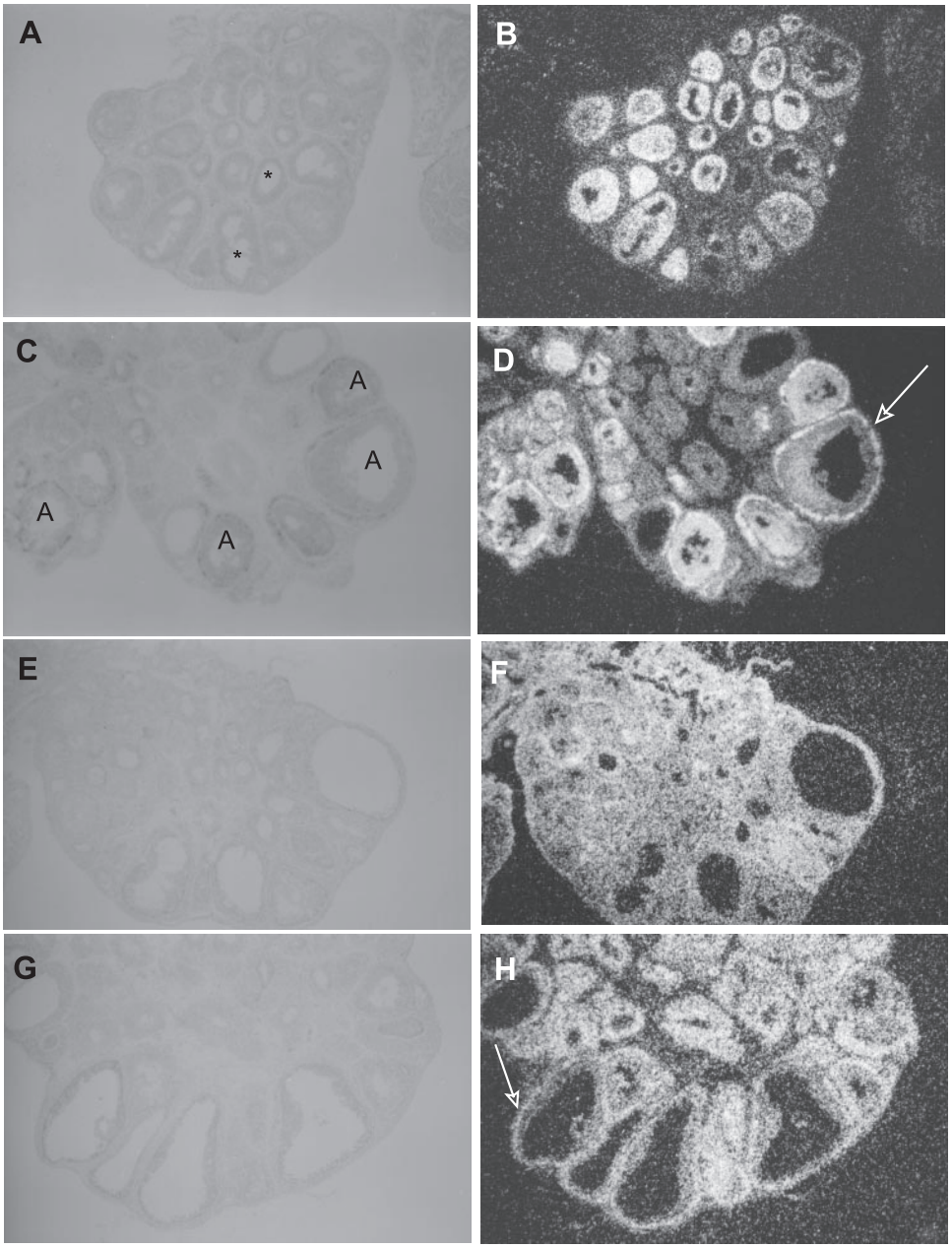

Fig. 3. Effect of PMSG on intraovarian localization of GCL subunit mRNA. Animals were treated as for Fig. 2. Ovaries were processed for in situ hybridization using antisense riboprobes for *gclc* and *gclm,* as detailed in MATERIALS AND METHODS. *A, C, E,* and *G*: bright-field views of ovaries from saline-treated (*A* and *E*) and PMSG-treated (*C* and *G*) animals. *B, D, F,* and *H*: dark-field views of the same fields as in *A, C, E*, and *G*. *B* and *D*: hybridization with *gclm* antisense riboprobe. *F* and *H*: hybridization with *gclc* antisense riboprobe. Original magnification ×13.2. *Atretic follicles have minimal *gclm* probe hybridization in granulosa cells. A, representative antral follicles. Arrows point to representative theca cell hybridization.

Effect of Ovulatory Dose of hCG on Whole Ovary GCL Protein and mRNA Expression and Intraovarian Localization of GCL Subunit mRNA in PMSG-Primed Rats

Ovarian GSH and GSSG and serum estradiol and progesterone concentrations. There were no significant changes in ovarian total GSH or in GSSG concentrations after hCG treatment (Fig. 4*A*). Serum estradiol levels declined and serum progesterone levels increased (Table 2), consistent with the previously described time course of changes in ovarian progesterone and estradiol levels after hCG (8). Ovarian weights also increased significantly (Table 2).

Ovarian GCL protein and mRNA levels. The changes in protein levels of both GCL subunits normalized to β-actin after hCG injection were qualitatively similar to the changes in the respective mRNAs, with very divergent effects of hCG on the two subunits. GCLm protein levels increased about threefold at 4 h, declined to 1.5-fold above baseline by 6 h, and declined to baseline levels at 12 h after hCG ($P < 0.001$; Fig. 4*B*). GCLc protein declined slightly over the period of study ($P = 0.002$, effect of time after hCG).

Quantitation of *gclm* mRNA using a fluorogenic 5′-nuclease assay (real-time PCR) showed a 10-fold increase in *gclm* mRNA levels normalized to *gapdh* at 4 h after hCG, followed by a decline to threefold over baseline levels at 6 h, and a further decline to below baseline levels at 12 h ($P = 0.002$, effect of time after hCG). In contrast, *gclc* mRNA levels normalized to *gapdh* did not change significantly after hCG ($P = 0.072$, effect of time after hCG). The change in the *gclm* to *gclc* mRNA ratio, from 1.1 ± 0.2 at 0 h to 6.5 ± 2.1 at 4 h, and to 1.0 ± 0.4 at 12 h (Fig. 4*D*), highlights the divergent

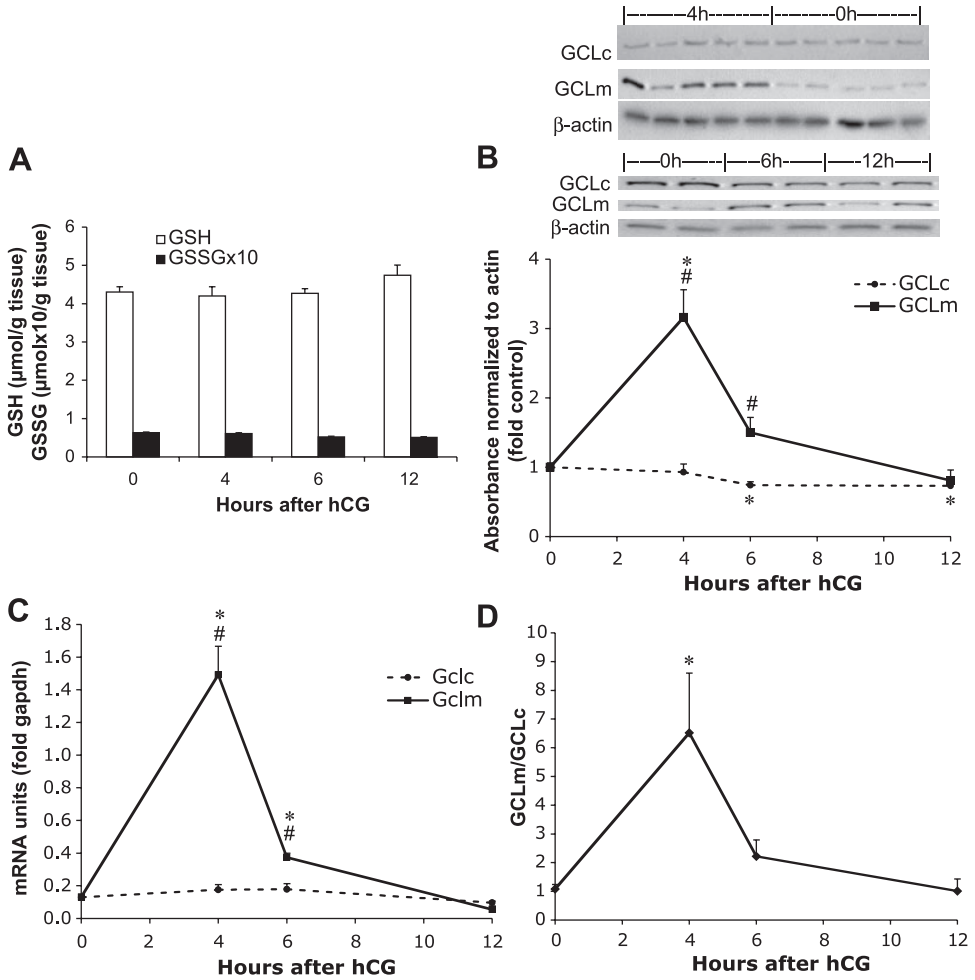

Fig. 4. Effect of ovulatory dose of human chorionic gonadotropin (hCG) on ovarian GSH concentrations and GCL subunit protein and mRNA levels in PMSG-primed rats. Prepubertal 23- to 24-day-old rats were injected sc with 10 IU PMSG. Some rats were killed 48 h later (0 h), others received an additional sc injection with 10 IU hCG and were killed 4, 6, or 12 h later. Ovaries were processed for GSH assay, protein extraction, and Western analysis or RNA extraction and real-time PCR for quantification of GCL mRNA, as detailed in MATERIALS AND METHODS. *A*: means ± SE total ovarian GSH concentration and (mean ± SE) x 10 glutathione disulfide (GSSG) concentration at various times after hCG injection (n = 5–11/group). Effect of time after hCG on GSH and GSSG, $P = 0.340$, $P = 0.183$, respectively. *B*: representative Western blots show GCLc, GCLm, and β-actin protein at indicated times after hCG injection. Graph shows mean ± SE absorbance values for GCLc and GCLm normalized to β-actin and expressed as fold control for the same blot (n = 5–10/group). Effect of time after hCG on GCLm and GCLc, $P < 0.001$, $P = 0.002$, respectively. *Statistically different from 0 h at $P < 0.05$ for a given GCL subunit; #statistically different from 12 h, $P < 0.05$. *C*: mean ± SE *gclc* or *gclm* mRNA level normalized to *gapdh* (n = 3–8/group). Effect of time after hCG on *gclm* and *gclc*, $P = 0.002$, $P = 0.084$, respectively. **gclm* Statistically different from 0 h, $P < 0.05$; #*gclm* statistically different from 12 h, $P < 0.05$. *D*: means ± SE *gclm*-to-*gclc* mRNA ratio. Effect of time after hCG, $P = 0.009$. *Statistically different from 0 h and 12 h, $P < 0.05$.

effects of hCG on expression of the two subunits ($P = 0.009$, effect of time after hCG). We estimated the relative copy numbers of *gclm* and *gclc* mRNA present in the samples at the start of PCR using the equation derived by Wilkening and Bader (52): $N_0 = 1.12 \times 10^{10}/E^{CN}$, where N_0 is the initial copy number, 1.12×10^{10} is the number of copies of a PCR product at the crossing point; E is the PCR efficiency, and CN is the cycle number at the crossing point. The estimated number of copies of *gclm* relative to copies of *gclc* in the control (0 h) samples from two different experiments were 1.9 and 12.4, indicating that *gclm* mRNA was more abundant than *gclc* in the ovaries at 0 h.

Statistical analyses carried out on the nonnormalized data yielded essentially the same results as analyses on the normalized data for both mRNA and protein levels (data not shown).

Intraovarian localization of gclm and gclc mRNA. Expression of *gclm* mRNA expression at 0 h was prominent in oocytes and theca cells of secondary and antral follicles and in theca cells of preovulatory follicles (Fig. 5*B*). The lowest levels of *gclm* expression at 0 h were observed in the granulosa cells of preovulatory follicles (Fig. 5*B*). *gclc* mRNA expression at 0 h was highest in the theca cells of growing follicles (Fig. 6*B*). At 4 h after hCG (Fig. 5, *D, F,* and *H*), there was a pronounced increase in *gclm* mRNA expression in the mural granulosa cells of preovulatory follicles, with minimal or no increase in the cumulus cells (Fig. 5*H*). *gclm* mRNA expression also increased greatly in theca cells of growing and preovulatory follicles and in areas of interstitium (Fig. 5*F*). In contrast, granulosa cell *gclm* expression did not increase in primary, secondary, and smaller antral follicles.

Table 2. *Effects of hCG on ovarian weight and serum estradiol and progesterone concentrations in PMSG-primed immature rats*

	Time after hCG			
End point	0 h	4 h	6 h	12 h
Paired ovary weight, mg†	66.7±2.1	76.9±2.8*	114.9±7.7*	150.6±6.1*
Estradiol, pg/ml†	175.3±24.5	132.1±30.6	177.0±18.5	38.3±5.8*
Progesterone, ng/ml†	5.6±1.5	46.5±0.8*	50.7±1.3*	43.0±1.9*

Values are means ± SE; n = 7–16/group. hCG, human chorionic gonadotropin; PMSG, pregnant mare's serum gonadotropin. *Significantly different from 0 h control by Fisher's least significant difference (LSD) test. †Effect of time after hCG, $P \leq 0.002$.

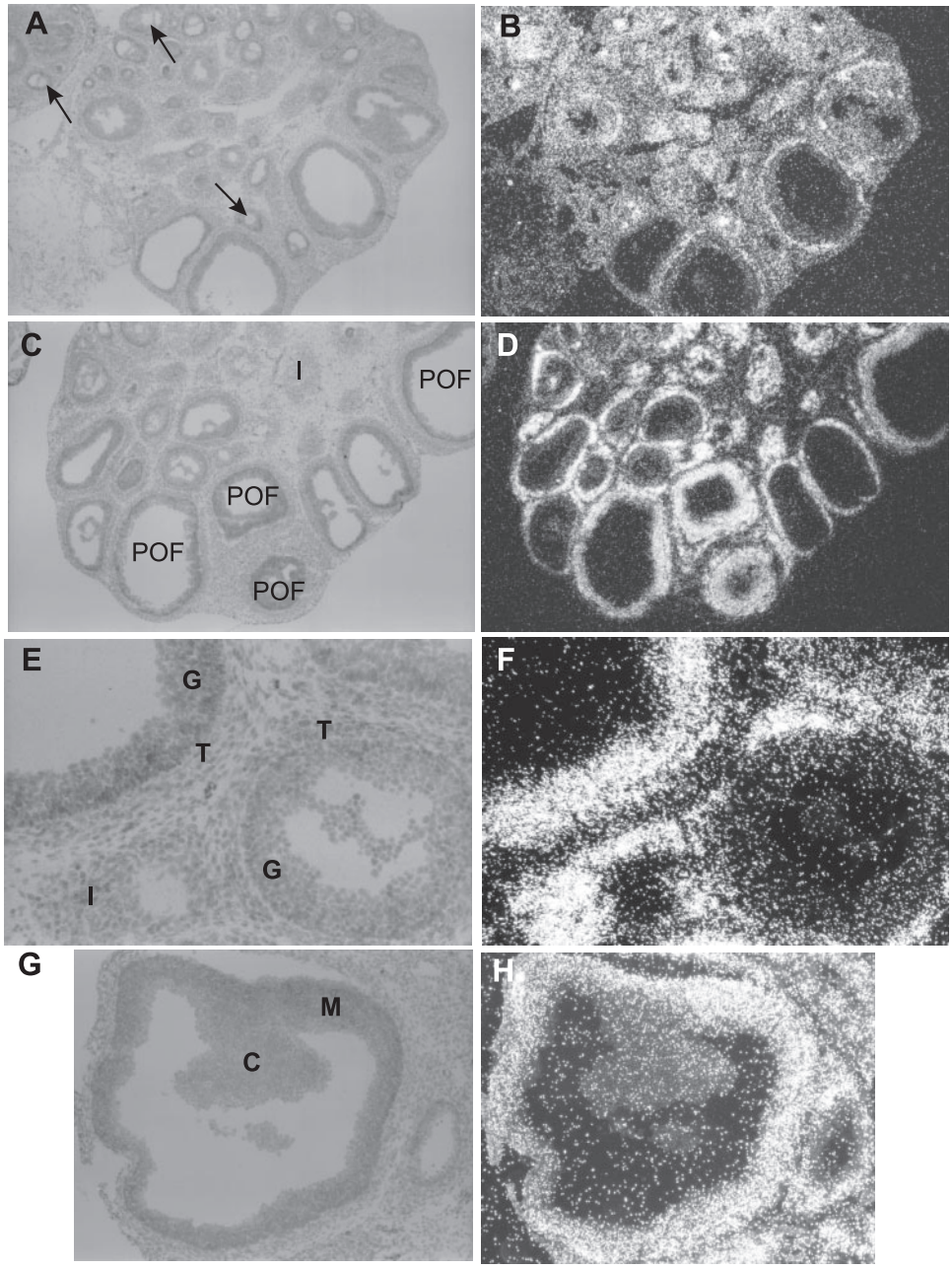

Fig. 5. Effect of ovulatory dose of hCG on intraovarian *gclm* mRNA expression. The experimental protocol was as for Fig. 4. Bright-field views of the same fields as the dark-field views showing hybridization with *gclm* antisense riboprobe are shown side by side. *A* and *B*: ovary from animal at 0 h shows strongest hybridization to theca cells and oocytes (latter indicated by arrows). Original magnification ×13.2. *C* and *D*: ovary from animal at 4 h after hCG shows increase in granulosa and theca cell hybridization in preovulatory follicles (POF), increased theca hybridization in growing follicles, and increased interstitial hybridization (I). Original magnification ×13.2. *E* and *F*: higher-power (original magnification ×66) view of ovary from animal at 4 h after hCG showing intense theca cell (T) hybridization in both preovulatory follicle and smaller antral follicle and intense granulosa cell (G) hybridization only in the preovulatory follicle. Interstitial hybridization (I) is also seen. *G* and *H*: higher-power (original magnification ×33) view of follicle from animal 4 h after hCG shows intense hybridization in mural granulosa cells (M) but not in cumulus cells (C).

At 6 h after hCG, *gclm* expression was qualitatively similar to 4 h, but less intense (data not shown). Ovarian *gclc* expression did not change among the various time points (Fig. 6, *B, D,* and *F*).

Effect of Endogenous Gonadotropin Surge on GCL Expression in the Ovary

Ovarian GSH. Total ovarian GSH concentrations increased between 0900 on proestrus and 0900 on estrus (Fig. 7*A*), as we have previously reported (28). Although the effect of estrous cycle time was not statistically significant by ANOVA ($P = 0.110$), a test for linear trend showed that ovarian GSH concentrations increased significantly between 0900 proestrus and 0900 estrus ($P = 0.027$).

Ovarian GCL subunit mRNA levels. Ovarian *gclm* mRNA levels were increased 3.5-fold at 2200 compared with 0900 proestrus and declined below proestrous morning levels by 0900 on estrus (Fig. 7*B*). The effect of estrous cycle time was statistically significant by ANOVA ($P = 0.006$), with post hoc tests showing that *gclm* mRNA levels at 0900 and 2200 proestrus and at 0000 estrus were significantly higher than at 0900 on estrus. Ovarian *gclc* mRNA levels declined between 0900 proestrus and 0900 estrus (Fig. 7*B*; $P = 0.048$, effect of time). The *gclm*-to-*gclc* mRNA ratio increased significantly at 2200 proestrus compared with the other time points ($P = 0.022$, effect of time).

Effect of PMSG and hCG on Ovarian GCL Enzymatic Activity

Ovarian GSH concentrations increased concomitantly with ovarian GCL enzymatic activity at 48 h after PMSG treatment

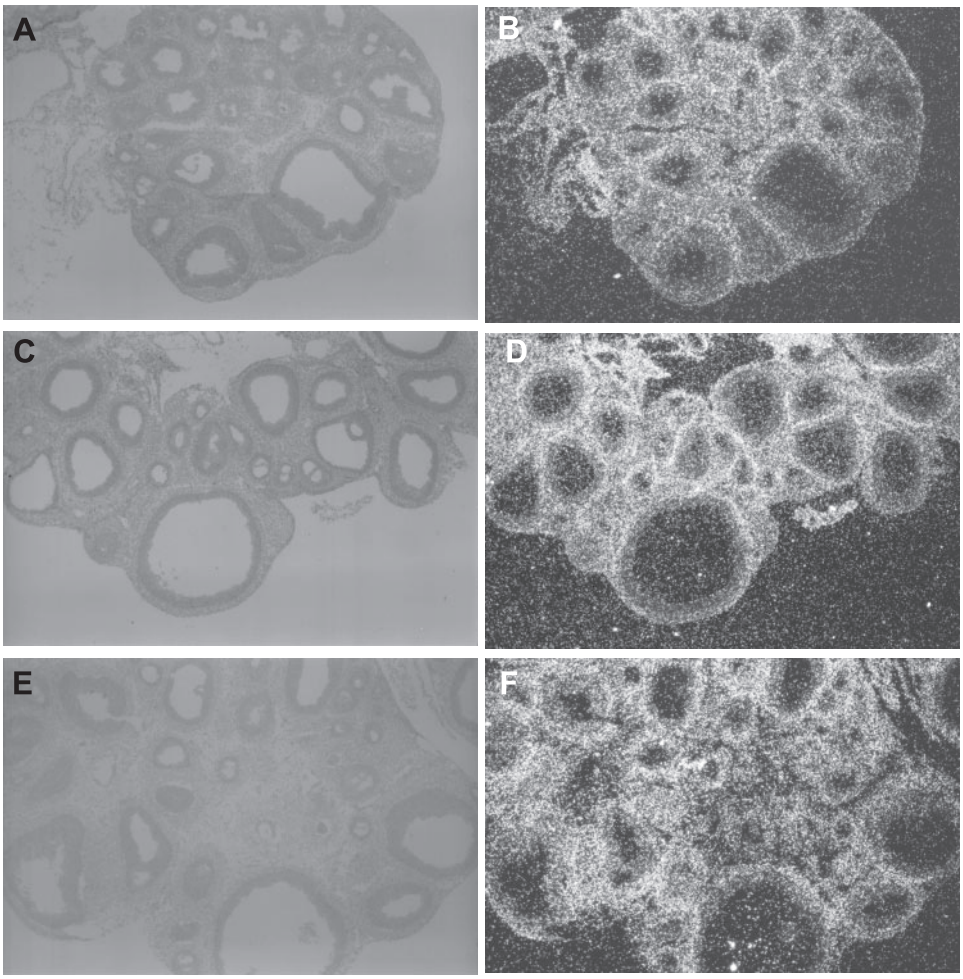

Fig. 6. Effect of ovulatory dose of hCG on intraovarian *gclc* mRNA expression. Bright-field views of the same fields as dark-field views showing hybridization with *gclc* antisense riboprobe are shown side by side. Ovaries from animals at 0 h (*A* and *B*), 4 h (*C* and *D*), and 6 h (*E* and *F*) after hCG treatment show no obvious changes in *gclc* riboprobe hybridization. Original magnification ×13.2.

(Table 3). Consistent with previous observations (3, 28), GSH concentration per milligram ovarian weight ($P < 0.001$, effect of treatment) and GSH concentration per milligram protein ($P = 0.011$, effect of treatment) increased at 48 h after PMSG compared with saline. There was no further increase at 4 h after hCG. Similarly, ovarian GCL enzymatic activity per milligram ovarian weight increased significantly at 48 h after PMSG administration compared with saline, with no further increase in GCL activity 4 h after hCG ($P = 0.046$, effect of treatment by ANOVA). In contrast, there was no increase in GCL activity per milligram protein at 48 h after PMSG or at 4 h after hCG ($P = 0.96$, effect of treatment by ANOVA).

DISCUSSION

Our results demonstrate that gonadotropins regulate ovarian synthesis of the antioxidant GSH by regulating expression of its rate-limiting enzyme GCL. We observed differential effects of gonadotropin on ovarian GCL subunit expression in follicles at different stages of development, on expression of GCLc vs. GCLm, and on GCL subunit protein expression vs. mRNA expression. During follicular growth induced by PMSG treatment, ovarian GCL protein levels, GCL enzymatic activity, and GSH concentrations increased without a concomitant increase in *gclm* mRNA levels and minimal increase in *gclc* mRNA levels. PMSG priming caused a shift in both *gclm* and *gclc* mRNA expression from a predominantly granulosa cell distribution to a predominantly theca cell distribution, as well as increases in follicular and interstitial GCLc protein expression. After hCG treatment in PMSG-primed rats, *gclm* mRNA expression increased dramatically in granulosa and theca cells of preovulatory follicles and in theca cells of growing follicles. Total ovarian GCLm mRNA and protein levels were increased by hCG in PMSG-primed rats and after an endogenous gonadotropin surge, without concomitant increases in GCLc. Neither ovarian GCL enzymatic activity nor ovarian GSH levels increased above PMSG-treated levels after hCG treatment.

Our observation of increases in GCLm protein and mRNA levels after an ovulatory gonadotropin stimulus without a concomitant increase in GCLc is an intriguing finding. Others have reported an increase in GCL mRNA levels peaking at 4 h after hCG by Northern blotting; however, it was not specified which GCL subunit was measured (7). GCLm is not known to possess functionality alone; it is known to heterodimerize with GCLc to increase the K_i for GSH and decrease the K_m for glutamate, leading to increased enzymatic activity of GCLc (13, 45). Our real-time PCR results show that, 48 h after PMSG, ovarian *gclm* mRNA is somewhat more abundant than *gclc* mRNA, suggesting that increasing *gclm* alone will not increase levels of GCL holoenzyme unless the two subunits are translated at different rates. Our Western blotting data show that, like the mRNA, GCLm protein increased after hCG, whereas GCLc protein did not. Ovarian GCL enzymatic activ-

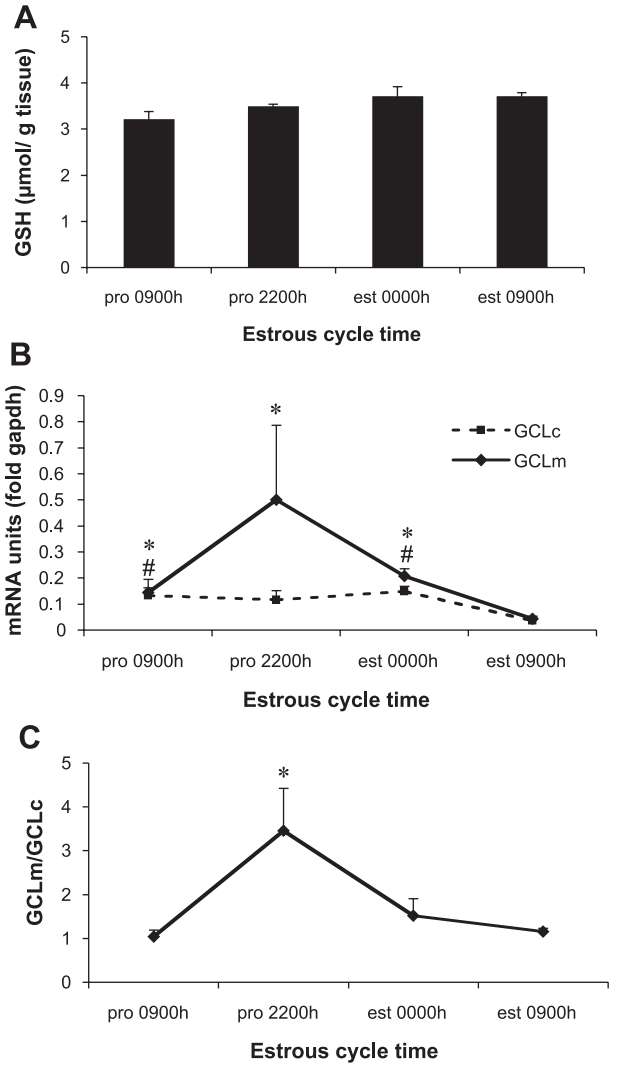

Fig. 7. Effect of endogenous gonadotropin surge on ovarian GSH concentrations and GCL subunit mRNA levels. Adult rats displaying 4-day estrous cycles were killed at 0900 on proestrus, 2200 on proestrus (~4 h after endogenous gonadotropin surge), 0000 on estrus (~6 h after endogenous gonadotropin surge), or 0900 on estrus. Ovaries were processed for GSH assay or for RNA extraction and real-time PCR quantification of *gclc* and *gclm* mRNA, as detailed in MATERIALS AND METHODS. *A*: mean ± SE ovarian GSH concentrations ($n = 4$/group). Effect of estrous cycle time by ANOVA, $P = 0.110$; test for linear trend, $P = 0.027$. *B*: mean ± SE *gclc* or *gclm* mRNA level normalized to *gapdh* ($n = 4$/group). Effect of estrous cycle time on *gclc* and *gclm*, $P = 0.048$, $P = 0.006$, respectively. **gclm S*tatistically different from 0900h estrus, $P < 0.05$; #*gclc* statistically different from 0900 estrus, $P < 0.05$. *C*: mean ± SE *gclm*-to-*gclc* mRNA ratio. Effect of estrous cycle time by ANOVA, $P = 0.022$. *Statistically different from 0900 proestrus, 0000 estrus, and 0900 estrus.

ity and GSH concentrations did not increase after hCG treatment, suggesting that the increase in GCLm subunit expression did not result in higher levels of GCL holoenzyme. Future experiments will manipulate expression of GCLm alone in cell lines to investigate roles of this protein in the absence of GCLc.

Our results extend and add specificity to previous observations that GCL mRNA (subunit not specified) expression increased in granulosa and theca cells of preovulatory follicles 4 after hCG (7). Our observations from in situ hybridization using an antisense *gclm* riboprobe show a similar time course and localization pattern to those reported for "GCL" in that study. In contrast, our observations using an antisense *gclc* riboprobe show very different patterns. The upregulation of *gclm* expression in granulosa and theca cells of preovulatory follicles by hCG may constitute part of an antioxidative stress response within preovulatory follicles. Although we did not observe increased GCL enzymatic activity or GSH concentrations in whole ovary homogenates after hCG, it is possible that an increase in GSH synthesis was localized to preovulatory follicles. Future experiments will test the effect of hCG treatment on cultured PMSG-primed preovulatory follicles to evaluate this possibility. Similar to the present observations with *gclm* mRNA, manganese superoxide dismutase mRNA expression increases markedly in theca cells of preovulatory follicles after hCG administration in PMSG-primed rats (40). This antioxidant response may serve to limit potentially destructive effects of ROS generated by the periovulatory influx of leukocytes into the preovulatory follicle (14, 22).

The mechanism by which an hCG/LH stimulus upregulates *gclm* mRNA expression remains to be determined. LH receptors are present in theca cells of growing and preovulatory follicles, in granulosa cells of preovulatory follicles, and in interstitial cells (21), all the cell types in which we observed increased *gclm* mRNA expression after hCG administration. LH binding to its receptors on granulosa cells and theca cells is well known to activate the cyclic AMP-protein kinase A intracellular signaling pathway (10). Neither the rat *gclc* promoter nor the rat *gclm* promoter contains a cyclic AMP response element (53, 54), suggesting that cyclic AMP response element-binding protein (CREB)-mediated regulation is not the mechanism that increases *gclm* transcription. It was recently reported that estrogen regulates antioxidant response element (ARE)-mediated gene transcription (2). AREs are important in transcriptional regulation of the human and mouse *gclc* and *gclm* genes (30, 32, 44); however, they have not been found in the sequenced portions of the rat promoters (53, 54). Ansell et al. (2) found that estradiol downregulated ARE reporter gene expression in COS-1 cells and decreased glutathione-*S*-transferase and quinone reductase enzymatic activity

Table 3. *Ovarian GSH concentrations and GCL enzymatic activity: effects of PMSG priming and ovulatory dose of hCG in PMSG-primed immature rats*

End point	Saline, 48 h	PMSG, 48 h	PMSG, 48 h/hCG, 4 h
Baseline GSH, nmol/mg ovary†	1.23±0.04	1.92±0.07*	1.85±0.10*
Baseline GSH, nmol/mg protein‡	21.45±1.23	26.75±1.28*	26.78±1.37*
GCL activity, pmol GSH·mg ovary^{-1}·min^{-1}‡	56.61±4.56	73.76±4.90*	74.99±6.61*
GCL activity, nmol GSH·mg protein^{-1}·min^{-1}	0.99±0.10	1.02±0.07	1.01±0.10

Values are means ± SE; $n = 8$/group. GSH, glutathione. *Significantly different from saline control by Fisher's LSD test. †$P < 0.001$, effect of treatment by ANOVA. ‡$P < 0.05$, effect of treatment by ANOVA.

in mouse uterus in vivo. They found no significant effects of estradiol on these enzymes in other organs, but they did not measure activity in ovary. Estradiol has been reported to upregulate *gclc* mRNA expression in human MCF7 cells via an ARE-mediated mechanism (31). Estradiol has also been reported to increase uterine GSH concentrations in rats (46), but the effect on GCL was not examined in that study. In the in vivo model system used in the current studies, ovarian estradiol synthesis increases with follicular growth induced by PMSG and declines after hCG administration (Table 2 and Ref. 8). However, the time course of change in estradiol was different from that of *gclm* mRNA. We observed no increase in *gclm* mRNA levels after PMSG treatment but a dramatic increase in *gclm* mRNA levels at 4 h after hCG followed by declines at 6 and 12 h. In contrast, serum estradiol levels were maximal at 48 h after PMSG, remained elevated at 4 and 6 h after hCG, and declined at 12 h after hCG. Another possibility is that the stimulatory effects of hCG on *gclm* expression are mediated by IGF-I. Insulin upregulates *gclc* expression, but not *gclm* or glutathione synthetase expression, in cultured rat hepatocytes (4, 17). Gonadotropins and estradiol stimulate granulosa cell production of IGF-I (16).

In contrast to the increase in both GCLm mRNA and protein levels observed after an ovulatory gonadotropin stimulus, stimulation of follicular development by PMSG increased ovarian GCLc and GCLm protein levels and GCL enzymatic activity without increasing *gclm* mRNA levels and only minimally increasing *gclc* mRNA levels (present studies and Ref. 28). These results are consistent with the conclusion that the increasing ovarian GCLc and GCLm protein levels observed at 8, 24, and 48 h after PMSG are likely caused by posttranscriptional effects of PMSG on GCL subunits. An increase in protein levels in the absence of an increase in mRNA levels could be due to increased translation or decreased degradation of GCLc and GCLm. Experiments are currently ongoing in our laboratory to determine whether gonadotropin suppresses GCL protein degradation or increases translation. The rate of protein degradation could be affected by alterations in ubiquitylation. Effects of gonadotropins on ubiquitin-related proteins have been reported. For example, granulosa cell levels of small ubiquitin-related modifier-1 protein are decreased at 48 h after PMSG administration (43). Recent evidence also shows that both LH and FSH can alter translation of some proteins without affecting their transcription. LH was reported to downregulate the rate of translation of connexin-43 in cultured ovarian follicles by a mechanism involving both protein kinase A and mitogen-activated protein kinase signaling (19). FSH stimulation increased translation of hypoxia-inducible factor-1 in granulosa cells by a mechanism involving phosphatidylinositol 3-kinase/Akt signaling (1).

We have demonstrated herein that, during follicular growth stimulated by PMSG, ovarian GSH concentrations, GCL subunit protein levels, and GCL enzymatic activity increase without a concomitant increase in GCL subunit mRNA levels. Within the ovary, PMSG treatment increases follicular GCLc protein in growing follicles. In contrast, an ovulatory gonadotropin stimulus in PMSG-primed rats dramatically increases ovarian *gclm* mRNA and protein levels without a concomitant increase in ovarian GCLc expression, GCL enzymatic activity, or GSH concentrations. We also showed that an ovulatory LH stimulus upregulates *gclm* mRNA expression, but not *gclc* mRNA, in mural granulosa cells and theca cells of preovulatory follicles and in theca cells of growing follicles. Thus *gclc* and *gclm* expression are differentially regulated by an ovulatory gonadotropin stimulus, and *gclm* expression is differentially regulated in follicles of different stages by an ovulatory gonadotropin stimulus. Our results also show that ovarian GSH synthesis is tightly regulated via gonadotropin stimulation of protein and/or mRNA expression of its rate-limiting enzyme in a follicle stage-dependent manner.

ACKNOWLEDGMENTS

We thank Jennifer Lavorin for assistance with the experiment on the effects of PMSG on ovarian GSH synthesis. We also thank Dr. Patricia Janssen of the Functional Genomics Laboratory, Department of Environmental and Occupational Health Sciences at the University of Washington for expert technical assistance in performing the fluorogenic 5′-nuclease assays. We also thank Dr. Fred Farin, Director of the Functional Genomics Laboratory.

Portions of this work were previously presented in abstract form at the Annual Meeting of the Society of Toxicology in 2003 and at the Annual Meeting of the Society for the Study of Reproduction in 2004.

GRANTS

This research was supported by Grant No. K08 ES-10963 from the National Institute of Environmental Health Sciences to U. Luderer, by the Center for Occupational and Environmental Health, University of California, Irvine, and by a UC Irvine Undergraduate Research Opportunities Program Fellowship to J. Lavorin.

REFERENCES

1. **Alam H, Maizels ET, Park Y, Ghaey S, Feiger ZJ, Chandel NS, and Hunzicker-Dunn M.** Follicle-stimulating hormone activation of hypoxia-inducible factor-1 by the phosphatidylinositol 3-kinase/Akt/Ras homolog enriched in brain (Rheb)/mammalian target of rapamycin (mTOR) pathway is necessary for induction of select protein markers of follicular differentiation. *J Biol Chem* 279: 19431–19440, 2004.
2. **Ansell PJ, Espinosa-Nicholas C, Curran EM, Judy BM, Philips BJ, Hannink M, and Lubahn DB.** In vitro and in vivo regulation of antioxidant response element-dependent gene expression by estrogens. *Endocrinology* 145: 311–317, 2003.
3. **Aten RF, Duarte KM, and Behrman HR.** Regulation of ovarian antioxidant vitamins, reduced glutathione, and lipid peroxidation by luteinizing hormone and prostaglandin F_{2alpha}. *Biol Reprod* 46: 401–407, 1992.
4. **Cai J, Sun WM, and Lu SC.** Hormonal and cell density regulation of hepatic gamma-glutamylcysteine synthetase gene expression. *Mol Pharmacol* 48: 212–218, 1995.
5. **Deneke SM and Fanburg BL.** Regulation of cellular glutathione. *Am J Physiol Lung Cell Mol Physiol* 257: L163–L173, 1989.
6. **Diaz D, Kresja CM, and Kavanagh TJ.** Localization of glutamate-cysteine ligase mRNA and protein in mouse kidney and induction with methylmercury. *Toxicol Lett* 123: 33–41, 2001.
7. **Espey LL and Richards JS.** Temporal and spatial patterns of ovarian gene transcription following an ovulatory dose of gonadotropin in the rat. *Biol Reprod* 67: 1662–1670, 2002.
8. **Espey LL, Tanaka N, Adams RF, and Okamura H.** Ovarian hydroxyeicosatetraenoic acids compared with prostanoids and steroids during ovulation in rats. *Am J Physiol Endocrinol Metab* 260: E163–E169, 1991.
9. **Gamcsik MP, Dolan ME, Andersson BS, and Murray D.** Mechanisms of resistance to the toxicity of cyclophosphamide. *Curr Pharm Des* 5: 587–605, 1999.
10. **Gore-Langton RE and Armstrong DT.** Follicular steroidogenesis and its control. In: *The Physiology of Reproduction* (2nd ed.), edited by Knobil E and Neill JD. New York: Raven, 1994, p. 571–627.
11. **Griffith OW.** Biologic and pharmacologic regulation of mammalian glutathione synthesis. *Free Radic Biol Med* 27: 922–935, 1999.
12. **Griffith OW.** Determination of glutathione and glutathione disulfide using glutathione reductase and 2-vinylpyridine. *Anal Biochem* 106: 207–212, 1980.
13. **Griffith OW and Mulcahy RT.** The enzymes of glutathione synthesis: gamma-glutamylcysteine synthetase. *Adv Enzymol Relat Areas Mol Biol* 73: 209–267, 1999.

14. **Hellberg P, Thomsen P, Janson PO, and Brännström M.** Leukocyte supplementation increases the luteinizing hormone-induced ovulation rate in the in vitro-perfused rat ovary. *Biol Reprod* 44: 791–797, 1991.
15. **Hornsby PJ and Crivello JF.** The role of lipid peroxidation and biological antioxidants in the function of the adrenal cortex. Part 2. *Mol Cell Endocrinol* 30: 123–147, 1983.
16. **Hsu CJ and Hammond JM.** Gonadotropins and estradiol stimulate immunoreactive insulin-like growth factor-I production by porcine granulosa cells in vitro. *Endocrinology* 120: 198–207, 1987.
17. **Huang ZA, Yang H, Chen C, Zeng Z, and Lu SC.** Inducers of gamma-glutamylcysteine synthetase and their effects on glutathione synthetase expression. *Biochim Biophys Acta* 1493: 48–55, 2000.
18. **Jernström B, Funk M, Frank H, Mannervik B, and Seidel A.** Glutathione-s-transferase A1–1-catalysed conjugation of bay and fjord region diol epoxides of polycyclic aromatic hydrocarbons with glutathione. *Carcinogenesis* 17: 1491–1498, 1996.
19. **Kalma Y, Granot I, Galiani D, Barash A, and Dekel N.** Luteinizing hormone-induced connexin 43 down-regulation: inhibition of translation. *Endocrinology* 145: 1617–1624, 2004.
20. **Kang Y, Qiao X, Jurma O, Knusel B, and Andersen JK.** Cloning/brain localization of mouse glutamylcysteine synthetase heavy chain mRNA. *Neuroreport* 8: 2053–2060, 1997.
21. **Kishi H and Greenwald GS.** Autoradiographic analysis of follicle-stimulating hormone and human chorionic gonadotropin receptors in the ovary of immature rats treated with equine chorionic gonadotropin. *Biol Reprod* 61: 1171–1176, 1999.
22. **Kodaman PH and Behrman HR.** Endocrine-regulated and protein kinase C-dependent generation of superoxide by rat preovulatory follicles. *Endocrinology* 142: 687–693, 2001.
23. **Laloraya M, Kumar PG, and Laloraya MM.** Changes in the levels of superoxide anion radical and superoxide dismutase during the estrous cycle of *Rattus norvegicus* and induction of superoxide dismutase in rat ovary by lutropin. *Biochem Biophys Res Commun* 157: 146–153, 1988.
24. **Li S, Thompson SA, Kavanagh TJ, and Woods JS.** Localization by in situ hybridization of gamma-glutamylcysteine synthetase mRNA expression in rat kidney following acute methylmercury treatment. *Toxicol Appl Pharmacol* 141: 59–67, 1996.
25. **Licht P, Bona Gallo A, Aggarwal BB, Farmer SW, Castelino JB, and Papkoff H.** Biological and binding activities of equine pituitary gonadotrophins and pregnant mare serum gonadotrophin. *J Endocrinol* 83: 311–322, 1979.
26. **Lopez SG and Luderer U.** Effects of cyclophosphamide and buthionine sulfoximine on ovarian glutathione and apoptosis. *Free Radic Biol Med* 36: 1366–1377, 2004.
27. **Luderer U, Diaz D, Faustman EM, and Kavanagh TJ.** Localization of glutamate cysteine ligase subunit mRNA within the rat ovary and relationship to follicular atresia. *Mol Reprod Dev* 65: 254–261, 2003.
28. **Luderer U, Kavanagh TJ, White CC, and Faustman EM.** Gonadotropin regulation of glutathione synthesis in the rat ovary. *Reprod Toxicol* 15: 495–504, 2001.
29. **Margolin Y, Aten RF, and Behrman HR.** Antigonadotropic and antisteroidogenic actions of peroxide in rat granulosa cells. *Endocrinology* 127: 245–250, 1990.
30. **Moinova HR and Mulcahy RT.** An electrophile responsive element regulates β-naphthoflavone induction of the human γ-glutamylcysteine synthetase regulatory subunit gene. *J Biol Chem* 273: 14683–14689, 1998.
31. **Montano MM, Deng H, Liu M, Sun X, and Singal R.** Transcriptional regulation by the estrogen receptor of antioxidative stress enzymes and its functional implications. *Oncogene* 23: 2442–2453, 2004.
32. **Mulcahy RT, Wartman MA, Bailey HH, and Gipp JJ.** Constitutive and β-naphthoflavone-induced expression of the human γ-glutamylcysteine synthetase heavy subunit gene is regulated by a distal antioxidant response element/TRE sequence. *J Biol Chem* 272: 7445–7454, 1997.
33. **National Research Council.** *Guide for the Care and Use of Laboratory Animals*. Washington, DC: NRC, National Academy of Sciences, 1996.
34. **Ogren L and Talamantes F.** The Placenta as an endocrine organ: polypeptides. In: *The Physiology of Reproduction*, edited by Knobil E and Neill JD. New York: Raven, 1994, p. 875–945.
35. **Pedersen T and Peters H.** Proposal for a classification of oocytes in the mouse ovary. *J Reprod Fertil* 17: 555–557, 1968.
36. **Peltola V, Huhtaniemi I, Metsa-Ketela T, and Ahotupa M.** Induction of lipid peroxidation during steroidogenesis in the rat testis. *Endocrinology* 137: 105–112, 1996.
37. **Plowchalk DR, Smith BJ, and Mattison DR.** Assessment of toxicity to the ovary using follicle quantitation and morphometrics. In: *Female Reproductive Toxicology*, edited by Heindel JJ and Chapin RE. San Diego, CA: Academic, 1993, p. 57–68.
38. **Reid LL, Botta D, Lu Y, Gallagher EP, and Kavanagh TJ.** Molecular cloning and sequencing of the cDNA encoding the catalytic subunit of mouse glutamate-cysteine ligase. *Biochim Biophys Acta* 26: 233–237, 1997.
39. **Reid LL, Botta D, Shao J, Hudson FN, and Kavanagh TJ.** Molecular cloning and sequencing of the cDNA encoding mouse glutamate-cysteine ligase regulatory subunit. *Biochim Biophys Acta* 1353: 107–110, 1997.
40. **Sadaki J, Sato EF, Nomura T, Mori H, Watanabe S, Kanda S, Watanabe H, Utsumi K, and Inoue M.** Detection of manganese superoxide dismutase mRNA in the theca interna cells of rat ovary during the ovulatory process by in situ hybridization. *Histochemistry* 102: 173–176, 1994.
41. **Sato EF, Kobuchi H, Edashige K, Takahashi M, Yoshioka T, Utsumi K, and MI.** Dynamic aspects of ovarian superoxide dismutase isozymes during the ovulatory process in the rat. *FEBS Lett* 303: 121–125, 1992.
42. **Seidel A, Friedberg T, Löllman B, Schwierzok A, Funk M, Frank H, Holler R, Oesch F, and Glatt H.** Detoxification of optically active bay- and fjord-region polycyclic aromatic hydrocarbon dihydrodiol epoxides by human glutathione transferase P1–1 expressed in chinese hamster V79 cells. *Carcinogenesis* 19: 1975–1981, 1998.
43. **Shao R, Zhang FP, Rung E, Palvimo JJ, Huhtaniemi I, and Billig H.** Inhibition of small ubiquitin-related modifier-1 expression by luteinizing hormone receptor stimulation is linked to induction of progesterone receptor during ovulation in mouse granulosa cells. *Endocrinology* 145: 384–392, 2004.
44. **Solis WA, Dalton TP, Dieter MZ, Freshwater S, Harrer JM, He L, Shertzer HG, and Nebert DW.** Glutamate-cysteine ligase modifier subunit: mouse gclm gene structure and regulation by agents that cause oxidative stress. *Biochem Pharmacol* 63: 1739–1754, 2002.
45. **Soltaninassab SR, Sekhar KR, Meredith MJ, and Freeman ML.** Multi-faceted regulation of γ-glutamylcysteine synthetase. *J Cell Physiol* 182: 163–170, 2000.
46. **Suojanen JN, Gay RJ, and Hilf R.** Influence of estrogen on glutathione levels and glutathione-metabolizing enzymes in uteri and R3230AC mammary tumors of rats. *Biochim Biophys Acta* 630: 485–496, 1980.
47. **Thompson SA, White CC, Krejsa CM, Diaz D, Woods JS, Eaton DL, and Kavanagh TJ.** Induction of glutamate-cysteine ligase (γ-glutamylcysteine synthetase) in the brains of adult female mice subchronically exposed to methylmercury. *Toxicol Lett* 110: 1–9, 1999.
48. **Tilly JL, Billig H, Kowalski KI, and Hsueh AJW.** Epidermal growth factor and basic fibroblast growth factor suppress the spontaneous onset of apoptosis in cultured rat ovarian granulosa cells and follicles by a tyrosine kinase-dependent mechanism. *Mol Endocrinol* 6: 1942–1950, 1992.
49. **Tilly JL and Tilly KI.** Inhibitors of oxidative stress mimic the ability of follicle-stimulating hormone to suppress apoptosis in cultured rat ovarian follicles. *Endocrinology* 136: 242–252, 1995.
50. **White CC, Viernes H, Kresja CM, Botta D, and Kavanagh TJ.** Fluorescence-based microtiter plate assay for glutamate-cysteine ligase activity. *Anal Biochem* 318: 175–180, 2003.
51. **Wilcox JN, Gee CE, and Roberts JL.** In situ cDNA:mRNA hybridization: development of a technique to measure mRNA levels in individual cells. In: *Neuroendocrine Peptides*, edited by Conn PM. New York: Academic, 1986, p. 510–533.
52. **Wilkening S and Bader A.** Quantitative real-time polymerase chain reaction: methodical analysis and mathematical model. *J Biomol Tech* 15: 107–111, 2004.
53. **Yang H, Wang J, Huang ZZ, Ou X, and Lu SC.** Cloning and characterization of the 5′-flanking region of the rat glutamate-cysteine ligase catalytic subunit. *Biochem J* 285: 476–482, 2001.
54. **Yang H, Wang J, Ou X, Huang ZZ, and Lu SC.** Cloning and analysis of the rat glutamate-cysteine ligase modifier subunit promoter. *Biochem Biophys Res Commun* 285: 476–482, 2001.